

Integrated mechatronic design of precision and energy saving electro-hydraulic systems

Bin Yao

School of Mechanical Engineering, Purdue University, West Lafayette, IN47907, USA

Kuang-piu Professor, The State Key Lab of Fluid Power Transmission and Control

Zhejiang University, Hangzhou, Zhejiang, 310027, P. R. China

byao@purdue.edu

Abstract

Lower cost, higher control performance and significantly less energy consumption are the goals for the design of any industrial systems including electro-hydraulics. The paper presents an integrated mechatronic design approach – seamless integration of advanced control techniques with novel hardware reconfiguration/re-design – as one of the tools to achieve these lofty goals simultaneously. The proposed integrated mechatronic design philosophy will be illustrated through recent research on the precision and energy saving control of electro-hydraulic systems. Specifically, instead of the traditional four-way valves, a unique configuration of five independently controlled poppet type cartridge valves is used as an example of hardware redesigns for the control of hydraulic systems. Such a hardware redesign not only enables decoupled controls of the meter-in and meter-out flows but also precise control of the cross-port regeneration flow for significant energy-savings. In addition, the much faster responses of the poppet type cartridge valves also provide the hardware capability of completely overcoming the performance limiting sandwiched deadband control problems associated with the traditional four-way proportional directional valves. Coordinated advanced adaptive robust controls are subsequently developed to effectively handle the increased complexity of system level controls and the difficulty of precisely controlling each individual cartridge valve due to the lack of accurate flow models. Comparative experimental results obtained have demonstrated that the proposed low cost programmable valves not only achieve significant energy saving but also higher control performance.

Keywords

Electro-Hydraulics, Valves, Energy saving, Adaptive robust control, Mechatronics

1 Introduction

Electro-hydraulic systems are traditionally controlled by four-way spool-type valves, either servo valves or proportional directional control (PDC) valves. Significantly large amount of research have been done recently to improve the electro-hydraulic system performance by applying advanced nonlinear adaptive and robust control techniques to deal with the hydraulic and mechanical nonlinearities (see references in [20]). All the works presented were rooted on electro-hydraulic systems controlled by the traditionally four-way spool type valves and purely from control points of view. Though the performances of those electro-hydraulic systems were significantly improved, no considerations were given to other practically important objectives such as reducing energy consumptions. Without some fundamental changes to the overall electro-hydraulic system design, it is even impossible to make a good tradeoff between the performance and the cost; better control performance has to be gained through the more expensive servo valves.

On the other hand, most fluid power engineers tend to solve problems with novel fluid power hardware designs only. It is thus no surprise that thousands types of valves and hydraulic components were developed and most of them have very narrow and specific applications. As a result, the design of industrial hydraulic systems becomes much more complex than the electro-mechanical systems, which has posted a significant challenge to the survival of fluid power industry. The situation becomes even worse when performance is concerned.

Instead of relying on only hardware or software via advanced controls alone, this paper re-approaches various issues from an integrated mechatronics design perspective, i.e., a balanced emphasis on both the hardware and software control designs in solving problems and in

making a better tradeoff among performance, cost and energy usage. Specifically, by knowing what advanced controls can do and cannot do, certain hardware re-design can be carried out to remove the performance limiting hardware barriers and/or to have a much simplified mechanical design for cost reduction even though the complexity of controlling the resulting system may increase. As has been verified through various application results [4,18,20], the proposed adaptive robust control [19] can effectively handle the effect of various smooth nonlinearities and uncertainties. As such, hardware designs do not have to focus on achieving a linear or a perfect known nonlinear input-output relationship. Instead, hardware designs should focus on solving the performance limiting hard nonlinearities such as deadband and backlash. In this regard, as will be detailed later in this paper, the use of cheap poppet type cartridge valves to replace the traditional four-way spool-type PDC valves when controlling an electro-hydraulic system serves as a perfect example of such a hardware redesign -- though the flow characteristics of cartridge valves cannot be modeled as precisely and simply as those of traditional PDC valves, the use of cartridge valves enables one to overcome the performance limiting deadband problems associated with the traditional PDC valves. In addition, such a hardware redesign significantly reduces the manufacturing cost as cartridge valves are known as economical alternatives to large PDC valves [16].

The hardware redesign often leads to a more capable physical system of increased flexibility and controllability, providing the hardware capability of achieving other practically meaningful goals in addition to better control performance (e.g., significantly reducing system energy usage). It is thus imperative to develop suitable advanced control strategies to make full use of those capabilities gained by hardware redesign. For example, the programmable valves consisting of five cartridge valves proposed in this paper eliminate the mechanical linkage between meter-in and meter-out flows and enable the precise control of regeneration flows. However, to make full use of these hardware capabilities, the recently developed advanced adaptive robust controls [19] have to be used since the simple linear control techniques used in the hydraulic industry cannot handle the large extent of uncertainties and the lack of suitable mathematical

models of cartridge valves, the main reason why cartridge valves have traditionally not been used in the precision control of electro-hydraulic systems.

The aim of this paper is to present a specific example of such an integrated mechatronic design approach – the energy saving precision control of electro-hydraulic systems based on the seamless integration of a novel hardware redesign via cheap cartridge valves and the advanced adaptive robust controls [21-22,10-11]. Comparative experimental results will be presented to demonstrate that the resulting mechatronic system not only achieves an improved control performance but also significantly reduces the system energy usage.

The rest of the paper is organized as follows. Section 2 introduces the configuration of the proposed programmable valves and details the motivations to its development. Section 3 focuses on the challenges in the control of programmable valves and the coordinated control of the energy saving electro-hydraulic systems. Section 4 presents the comparative experimental results and section 5 draws the conclusions from the study.

2 Energy Saving Programmable Valves

2.1 Ways to Reduce Energy Consumptions

The energy used by a hydraulic system to perform a task can be calculated as:

$$E = \int_{t_0}^{t_1} P_s(\tau)Q_s(\tau)d\tau \quad (1)$$

where t_0 and t_1 are the starting and the ending time of the task, and P_s and Q_s represent the supply pressure and the flow rate from the hydraulic pump. It is obvious that there exist two ways to reduce the energy usage:

1. *reduce the pump supply pressure $P_s(t)$*
2. *reduce the flow rate $Q_s(t)$ needed from a pump*

Without considering the fluid compressibility, the flow rate needed from a pump to perform a given task depends on the cylinder piston movement only and would be pretty much fixed unless additional flow paths such as the regeneration flows between the two chambers of the cylinder are created. To reduce the pump supply pressure, working pressures at the two cylinder chambers are desired to be as low as possible so long their pressure difference can be maintained at the level needed to perform the required motion. Therefore, independently

controlling flows to two chambers of a cylinder with additional flow paths such as the cross-port flows and having low working pressures for the two chambers without losing controllability and performance are the keys to reducing energy consumption for energy saving.

Traditionally, a four-way valve, either servo or PDC, is used to control each hydraulic cylinder as done in almost all existing publications [13,17,20,2]. With such a valve configuration the meter-in and meter-out orifices are mechanically linked and the flows to the two chambers of the cylinder cannot be independently regulated. Consequently only one of the two cylinder states (i.e., pressures of the two chambers) is completely controllable. There exists a one-dimensional internal dynamics [20] which cannot be modified by any input-output type control strategies. The control input to the valve in those strategies is uniquely determined once the desired motion is specified, which makes the regulation of individual cylinder chamber pressures impossible. As a result, though high system performance can be achieved with the use of advanced controls (e.g., [20]), significant reduction of energy consumption is unattainable.

The need to eliminate the mechanical linkage between the meter-in and meter-out orifices for independent regulation of two cylinder chamber flows is well known and has been used in heavy industrial applications. For example, the spool type valve is replaced by four poppet type valves in [8], and a number of slight variations exist throughout the mobile hydraulics industry [3]. Patents by various companies [7,9,1] attest to the potential of this technique. Specialized hardware such as the independent metering valves (IMV) shown in (a) of Fig. 1 by Caterpillar Inc. has also been developed, in which each metering valve is independently controlled, allowing completely separated controls of flows to two cylinder chambers.

As illustrated in (b) of Fig.1, another well-known technique to reduce energy usage is to make full use of the regeneration flows [7], i.e., the flow pumped from one chamber of the cylinder to the other chamber using energy of the external load (e.g., the potential energy of a load during downward motions and the kinematic energy of a load during deceleration motions). Flow regeneration is a highly efficient process in which little or zero pump flow or energy is needed. Ideally, regeneration should be

used whenever the external force is in the same direction as the desired motion for attaining maximum efficiency. The four-valve IMVs also enables the use of regeneration flow but not to the fullest extent possible [1]. The reason is that, unlike in (b) where a dedicated valve is used, a completely controllable cross port flow path is not available in IMVs since such a flow path has to be created by opening both valves connecting to either the return line to the tank or the pressurized line to the pump. Either scenario can happen only at certain extreme loading conditions. For example, to use the two valves connecting to the pressurized line for the cross port flow, the pressures of cylinder chambers should be higher than the pump supply pressure. Because of these, though significant energy saving could be achieved for operations such as free fall or dump, precise control of regeneration flows is normally unattainable and simultaneous good motion control performance cannot be accomplished with this set of hardware. Partly because of these difficulties, there have not been any published results on the simultaneous precise motion tracking and significant energy saving.

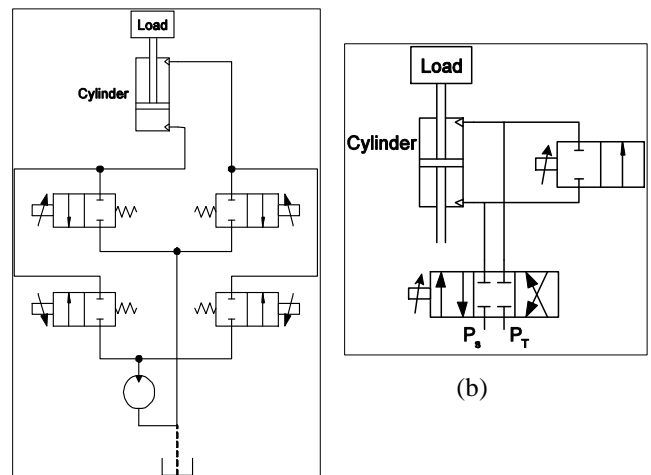


Fig.1: (a) Four valve IMVs (b) Regeneration flows

The author was exposed to the IMVs concept when he started his fluid power control research with Caterpillar Inc. The hardware advantages of IMVs over traditional spool type valves impressed him very much and he was determined to reap the hardware benefits of IMVs with the advanced adaptive robust controls he have developed over the years [18-20]. To make full use of the regeneration flows for maximum energy-saving while having a controlled motion, a fifth valve is added to the IMVs configuration to create the programmable valves

shown in Fig.2 and studied in [21-22,10-11]. It should be noted that such a configuration is used simply because it enables a completely controllable cross-port flow and can be built with off-the-shelf one-way valves such as the poppet type cartridge valves. As long as a completely controllable cross-port flow path and independent control of flows to the two chambers of a cylinder can be realized, other specialized hardware with possibly even less number of valves through well thought-out hardware integration can also be used.

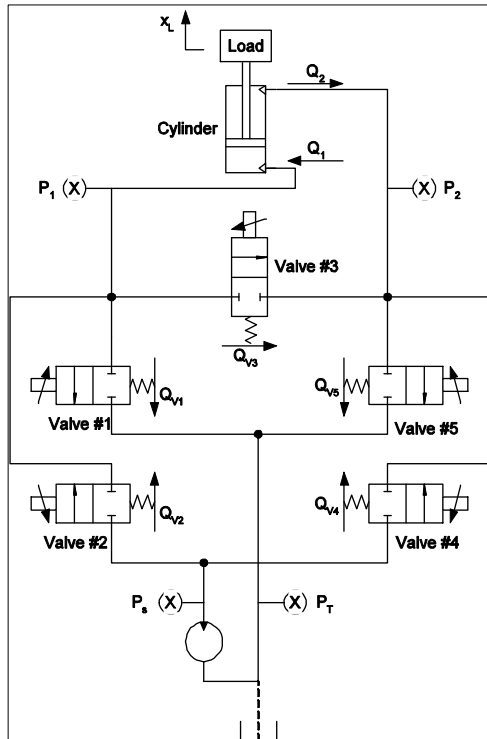


Fig. 2: Programmable valves configuration

2.2 Hardware Benefits of Programmable Valves

The five independently controlled one-way proportional valves in the proposed programmable valves provide the hardware capability of fully decoupled control of meter-in and meter-out flows and precise control of cross-port flows at any time. To further reduce manufacturing costs, poppet type proportional cartridge valves, which are known as economical alternatives to large proportional valves and have low maintenance costs [16], are used. In addition, cartridge valves are also known for their low leakage characteristics. For example, Vickers EPV10 series has a typical leakage of less than 3cc/min. Thus, aside from a higher degree of energy efficiency, the programmable valves can also be used as a load holding device when they are not in the energized

modes.

Aside from the cost benefits, the proposed programmable valves also have certain hardware advantages over the traditional spool type valves from a controls' perspective. Specifically, the much smaller inertia of the cartridge valves' moving parts leads to the much faster valve dynamic response; in fact, cartridge valves have been mainly used in hydraulic industry for various safety precaution measures due to their fast responses. This hardware benefit will significantly simplify the advanced controller designs and put much less restrictive limitations on the achievable closed-loop bandwidth – all existing advanced controllers with experimental verifications [2,4,20] have neglected the valve dynamics for simplicity, and consequently the achievable closed-loop bandwidth in implementation is limited by the bandwidth of the actual valve responses.

2.3 Solution to Performance Limiting Sandwiched Deadband Control Problems

Closed-center valves such as the proportional directional control (PDC) valves are widely used in industry for position or velocity control applications. An over-lapped spool shown in Fig.3 is intentionally used in these kinds of valves to prevent internal leakages during non-energized modes so that the closed-loop system can hold a position even when the power is off. Unfortunately, such an over-lapped spool also introduces a deadband between the spool displacement and the actual valve orifice opening and creates the so-called sandwiched deadband control problems shown in Fig.4 – the deadband is between the valve spool dynamics and the plant dynamics.

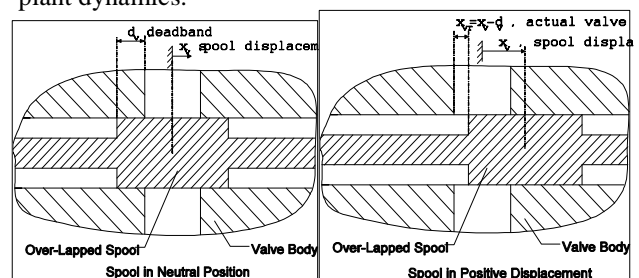


Fig. 3: Over-lapped closed-center PDC valves

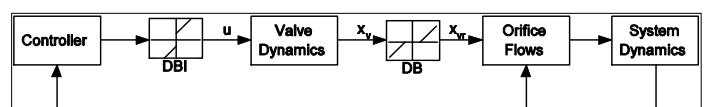


Fig. 4: Hydraulic systems controlled by PDC valves

It is well-known that the sandwiched deadband control problem is both theoretically and practically difficult to solve [15]. Even though the destabilizing effect of the deadband could be accounted for by suitable control designs, there will always exist a hard limitation on the achievable closed-loop control performance no matter what type of advanced controls to be used. For example, the traditional method is to use the direct inverse of the deadband nonlinearity shown in Fig. 4 to cancel the deadband effect [5-6,12]. Successful implementation of this strategy without closed-loop instability issues relies on two conditions: a) the deadband is known or accurately estimated, and b) the valve dynamics is fast enough to be neglected. The first condition may be achieved through off-line system identification [5], but the second condition can be satisfied only by limiting the achievable closed-loop system bandwidth low enough so that the valve dynamics (usually pretty slow for PDC valves) looks “faster enough” when compared with the closed-loop bandwidth. Though both feed-forward controller [5] and local high-gain feedback control [5,15] have been proposed to boost the valve dynamic response, in practice, neither method was able to improve the overall control performance significantly due to several implementation constraints as revealed by the experimental results in [5,12]. Specifically, the success of using the feed-forward controller heavily depends on the accuracy of the valve dynamics, while the local high-gain feedback controller needs the measurement of valve spool position, which tends to be too noisy to be of much usefulness, aside from the much increased system cost of having the spool position sensor. Because of these issues, PDC valves have not been used in hydraulic industry for precision motion controls. Instead, the critically centered or under-lapped servo valves are used at the expense of increased energy usage and the loss of the ability of holding positions when the valve is shut off due to significant leakage flows.

The poppet type cartridge valve, as shown in Fig. 5, also has deadband between the control input voltage to the valve and the resulting valve flow due to the fact that the input voltage has to be large enough to overcome the pre-load spring force and the static friction for the valve poppet to move to open the orifice. However, such a deadband is fundamentally different from the sandwiched deadband problem of PDC valves and can be easily

overcome by suitable controller designs. Specifically, the electrical dynamics between the commanded input voltage to the valve and the resulting electro-magnetic force are usually in kilo-Hz range. They are much higher than the PDC valve dynamics relating the valve input voltage to the spool displacement and can be safely neglected as in the precision control of electrical motors [18]. Therefore, as illustrated in Fig. 6 where the valve dynamics refers to the poppet dynamics between the net force acting on the poppet to its displacement, the deadband is of the input deadband type and can be easily canceled via the well-known deadband inverse [14]. Furthermore, as the poppet only moves uni-directionally, the deadband can be essentially removed by setting the right amount of input off-set. All these make it a hardware reality of bypassing the performance limiting sandwiched deadband problem of traditional spool valves, paving the way to achieve a higher control performance.

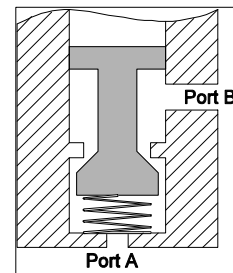


Fig. 5: Poppet type cartridge valves

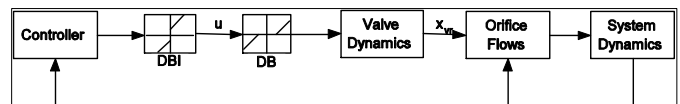


Fig. 6: Cartridge valve controlled hydraulic systems

3 Coordinated Control Strategy

As shown in Fig.2, the use of programmable valves provides the hardware capability of independently controlling the pressures of both chambers, P_1 and P_2 , and the control of the cross-port flow between the two chambers. However, it also increases the complexity of controlling the resulting system significantly. The difficulties of controlling such a system not only come from the well-known issues of highly nonlinear hydraulic dynamics and large extents of parameter variations and uncertain nonlinearities [13,20] but also from the lack of accurate mathematical model of cartridge valve flow characteristics and the need to coordinate the control of

the five cartridge valves.

How to effectively deal with nonlinearities and the large extents of parametric uncertainties and uncertain nonlinearities have been solved by applying the recently developed adaptive robust control (ARC) strategy in [20]. A schematic of the standard ARC controller structure is shown in Fig. 8, in which a robust feedback is synthesized via deterministic robust control techniques to guarantee global stability and certain robust performance of the closed loop system while a controlled on-line parameter estimation process is employed to reduce the effect of parametric uncertainties without affecting the robust stability and performance results by the robust feedback. The physical model based model compensation effectively takes into account of the system nonlinearities.

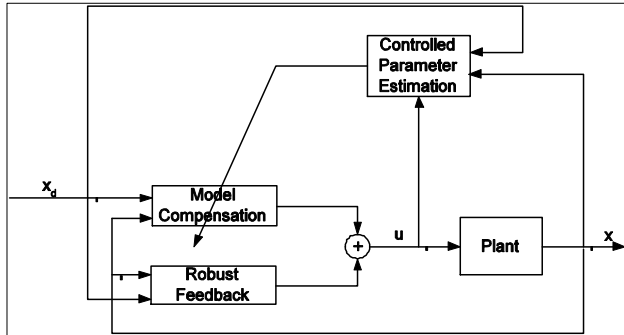


Fig. 7: Schematic of adaptive robust controls

The problem of lacking accurate mathematical model of the nonlinear cartridge valve flow mappings can be solved by using look-up tables that relate the valve flow rates to the valve input voltages and the pressure drops across the valve orifices. Such flow mapping tables can be obtained either by off-line experiments or through automated on-line modeling techniques in [11].

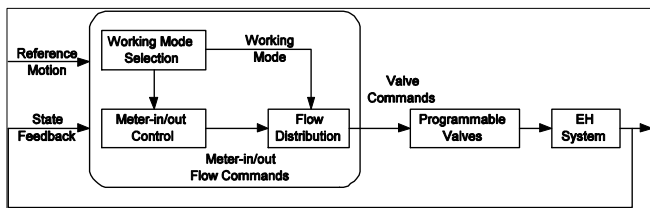


Fig. 8: Two-level control structure

The difficulties in the coordinated control of the five cartridge valves have been dealt with through a two-level controller structure shown in Fig. 8 in [22]. Specifically, given the current system states and desired motion trajectory, the task level controller determines the specific subsets of the programmable valves to be used which will enable maximal energy saving while without losing the

controllability for precise motion tracking. This process is normally referred to as the working mode selection in hydraulic industry. The valve level controllers use the adaptive robust control strategy to precisely regulate the pressures of both cylinder chambers under the chosen working mode to achieve the dual objectives of precise motion tracking and significant energy saving.

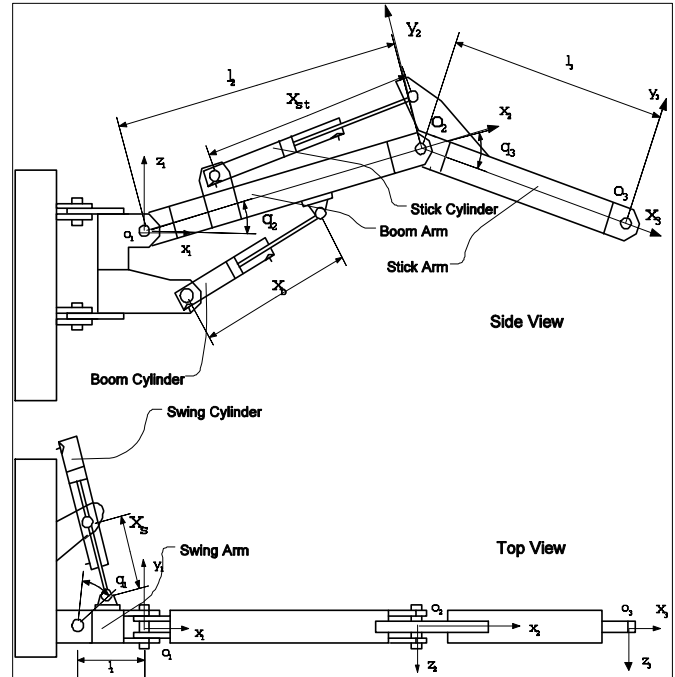


Fig. 9: A three DOF hydraulic robotic arm

To illustrate the effectiveness of the above strategies in practical applications, in the following, controlling the boom motion of a three degrees-of-freedom (DOF) electro-hydraulic robot arm using the proposed programmable valves will be presented. The system is built to mimic the industrial backhoe loader arms, which is detailed in [20]. With the coordinate systems, joint angles and physical parameters of the system defined in Fig. 9, the boom motion dynamics with the other two joints fixed can be described by [4,10]:

$$(J_C + m_L \ell_e^2) \ddot{q}_2 = \frac{\partial x_L}{\partial q_2} (P_1 A_1 - P_2 A_2) - G_C(q_2) - D_f \cdot \dot{q}_2 - m_L g \ell_g(q_2) + T(t, q_2, \dot{q}_2) \quad (2)$$

where q_2 represents the boom joint angle, x_L represents the boom cylinder displacement, J_C is the moment of inertia of the boom without payload, m_L represents the mass of the unknown payload, G_C is the gravitational load of the boom without payload, P_1 and P_2 are the head and rod end pressures of the cylinder

respectively, A_1 and A_2 are the head and rod end ram areas of the cylinder respectively, D_f is the viscous friction coefficient and T represents the lumped disturbance torque including external disturbances and terms like the unmodelled friction torque. The specific forms of J_C , $G_C(q_2)$, $\ell_g(q_2)$, and ℓ_e^2 are described in [4].

The moment of inertia and the gravity force both depend on the unknown payload m_L . For notational simplicity, they are split into two parts. The first parts, J_C and $G_C(q_2)$, are their values under no payload situation, and the second parts, the terms $m_L g \ell_g(q_2)$ and $m_L \ell_e^2$ are the additional values due to the unknown payload m_L . The second parts will be estimated on-line via certain parameter adaptation law specified later. Neglecting cylinder flow leakages, the hydraulic cylinder equations can be written as [20]:

$$\begin{aligned} \frac{V_1}{\beta_e} \dot{P}_1 &= -A_1 \dot{x}_L + Q_{1M} + \tilde{Q}_1 = -A_1 \frac{\partial x_L}{\partial q_2} \dot{q}_2 + Q_{1M} + \tilde{Q}_1 \\ \frac{V_2(x_L)}{\beta_e} \dot{P}_2 &= A_2 \dot{x}_L - Q_{2M} - \tilde{Q}_2 = A_2 \frac{\partial x_L}{\partial q_2} \dot{q}_2 - Q_{2M} - \tilde{Q}_2 \end{aligned} \quad (3)$$

where $V_1(x_L) = V_{h1} + A_1 x_L$ and $V_2(x_L) = V_{h2} - A_2 x_L$ are the total cylinder volumes of the head and rod ends including the connecting hose volumes respectively, V_{h1} and V_{h2} are the initial control volumes when $x_L = 0$, β_e is the effective bulk modulus, Q_{1M} and Q_{2M} are the supply and return flows respectively with \tilde{Q}_1 and \tilde{Q}_2 being the corresponding flow modeling errors. When the programmable valves are used to control the boom motion, Q_{1M} and Q_{2M} are given by:

$$\begin{aligned} Q_{1M} &= +Q_{v2} - Q_{v1} - Q_{v3} \\ Q_{2M} &= -Q_{v3} - Q_{v4} + Q_{v5} \end{aligned} \quad (4)$$

where Q_{vi} , $i=1,2,\dots,5$, is the orifice flow through the i -th cartridge valve. Due to the sufficiently fast response of the cartridge valves, one can neglect the valve dynamics and treat the cartridge valve flow as a static function of the orifice pressure drop ΔP_{vi} and the commanded valve input u_i by:

$$Q_{vi} = f_i(\Delta P_{vi}, u_i), \quad i=1,2,\dots,5 \quad (5)$$

where f_i represents the nonlinear orifice flow mapping. The dual objectives of this study can then be stated precisely as follows:

- **Performance:** Given the desired motion trajectory $q_d(t)$, the primary objective is to synthesize control signals for the five cartridge valves (i.e., u_{vi} , $i=1,\dots,5$)

such that the system output $q_2(t)$ tracks $q_d(t)$ as closely as possible in spite of various model uncertainties.

- **Energy Saving:** The secondary objective is to minimize the overall pump energy usage.

The following notations will be used throughout the paper. Let $\theta = [\theta_1, \theta_2, \dots, \theta_n]$ denote the vector of unknown parameters in the system dynamic equations, $\hat{\theta}$ the estimate of θ , and $\tilde{\theta}$ the estimation error (i.e., $\tilde{\theta} = \hat{\theta} - \theta$). Let $\theta_{max} = [\theta_{1max}, \theta_{2max}, \dots, \theta_{nmax}]$ and $\theta_{min} = [\theta_{1min}, \theta_{2min}, \dots, \theta_{nmin}]$ be the upper and lower bounds of the unknown parameter vector θ respectively, i.e., $\theta_{min} \leq \theta \leq \theta_{max}$, in which the operation $<$ for two vectors is performed in terms of the corresponding elements of the vectors. With known θ_{min} and θ_{max} , a discontinuous projection, $Proj_{\hat{\theta}}(\bullet) = [Proj_{\hat{\theta}_1}(\bullet_1), \dots, Proj_{\hat{\theta}_n}(\bullet_n)]^T$, can be defined as [19]:

$$Proj_{\hat{\theta}_i}(\bullet_i) = \begin{cases} 0, & \text{if } \hat{\theta}_i = \theta_{imax} \text{ and } \bullet_i > 0 \\ 0, & \text{if } \hat{\theta}_i = \theta_{imin} \text{ and } \bullet_i < 0 \\ \bullet_i, & \text{otherwise} \end{cases} \quad (6)$$

The following discontinuous projection based adaptation law will then be used in the ARC design:

$$\dot{\hat{\theta}} = Proj_{\hat{\theta}}(\Gamma \tau) \quad (7)$$

where Γ is a diagonal positive definite adaptation rate matrix and τ is an adaptation function specified later.

3.1 Working Mode Selection

Let $P_L = P_1 A_1 - P_2 A_2$ be the load force to actuate the cylinder rod. For precise motion tracking, it is necessary that P_L can be controlled accurately as well. When the traditional four way valves are used, the necessary load force profile P_L for the specified motion will uniquely determine the only control input to the valve. However, with the proposed programmable valves, due to the availability of five valve control inputs, infinite number of combinations of 5 valve inputs exist to provide the needed load force profile for motion tracking. It is thus desirable to choose a specific combination out of those so that P_1 and P_2 are as low as possible to reduce the needed pump supply pressure for energy saving. Furthermore, the regeneration flows should be used whenever possible to maximize the energy saving. With these in mind, the following strategy will be adopted: one

of the two cylinder chambers will be kept at a low pressure close to the return line tank pressure while controlling the other chamber's pressure precisely to provide the needed load force profile for motion tracking. In the following, the low pressure chamber will be referred to as the off-side while the other chamber as the working-side to represent the fact that controlling this chamber's pressure is critical to the precise motion tracking.

The working mode selection is task dependent. There are five tracking modes and three regulation modes. The tracking mode selection, shown in Table 1, is based on the desired cylinder velocity \dot{x}_d , the actual cylinder pressures P_1 and P_2 , and the desired load force P_{Lda} needed for precise motion tracking. The regulation mode selection is shown in Table 2, in which ε is a small preset positive number.

Table 1: Tracking Mode Selection

| \dot{x}_d | P_{Lda} | Valve Configuration | Offside | Mode |
|-------------|----------------------------|--|---------|-------|
| > 0 | > 0 | $Q_1 = Q_{v2}, Q_2 = Q_{v5}$ | P_2 | T_1 |
| > 0 | < 0 | $Q_1 = Q_{v2} - Q_{v3}$ $Q_2 = -Q_{v3}$ | P_1 | T_2 |
| < 0 | $> 0 \&$ $P_1 > P_2$ | $Q_1 = -Q_{v3}$ $Q_2 = Q_{v5} - Q_{v3}$ | P_2 | T_3 |
| < 0 | $> 0 \&$ $P_1 \leq P_2$ | $Q_1 = -Q_{v1}, Q_2 = -Q_{v4}$ | P_2 | T_4 |
| < 0 | < 0 | $Q_1 = -Q_{v1}, Q_2 = -Q_{v4}$ | P_1 | T_5 |

Table 2: Regulation Mode Selection

| \dot{x}_d | $x - x_d$ | Valve Configuration | Offside | Mode |
|-------------|-----------------|--|---------|-------|
| $= 0$ | $> \varepsilon$ | $Q_1 = -Q_{v3}$ $Q_2 = Q_{v5} - Q_{v3}$ | P_2 | R_1 |
| $= 0$ | $< \varepsilon$ | $Q_1 = Q_{v2}, Q_2 = Q_{v5}$ | P_2 | R_2 |
| $= 0$ | otherwise | $Q_1 = 0, Q_2 = 0$ | | R_3 |

3.2 Offside Pressure Regulator Design

The objective of the off-side pressure regulator is to keep the offside pressure at a constant low pressure P_0 close to the return line tank pressure. For simplicity, this section only presents the design of the pressure regulator for those working modes during which the offside chamber pressure is P_2 . The pressure regulator design for working modes with P_1 being the offside chamber pressure is the same and omitted.

The dynamics of P_2 is described in (3). In order to

use parameter adaptation to reduce parametric uncertainties to improve performance, it is necessary to linearly parameterize the system dynamics in terms of a set of unknown parameters. For this purpose, let θ_p be $\theta_p = [\theta_\beta, \theta_Q]^T$, where $\theta_\beta = \beta_e$ and $\theta_Q = \beta_e \tilde{Q}_{2n}$, in which \tilde{Q}_{2n} is the nominal value of \tilde{Q}_2 . The P_2 dynamics can thus be rewritten as:

$$\dot{P}_2 = \frac{A_2}{V_2} \frac{\partial x_L}{\partial q_2} \dot{q}_2 \theta_\beta - \frac{\theta_\beta}{V_2} Q_{2M} - \frac{\theta_Q}{V_2} + \Delta_{Q_2} \quad (8)$$

where $\Delta_{Q_2} = \beta_e (\tilde{Q}_{2n} - \tilde{Q}_2) / V_2$ represents the effect of time-varying portion of the flow modelling error \tilde{Q}_2 . It is assumed that the parameters and Δ_{Q_2} are bounded by some known bounds, which is realistic because both the bulk modulus β_e and the modelling error of the flow mapping are practically bounded. Denote the pressure regulation error as $e_{p2} = P_2 - P_0$. Then,

$$\dot{e}_{p2} = -\frac{\theta_\beta}{V_2} Q_{2M} + \frac{A_2}{V_2} \frac{\partial x_L}{\partial q_2} \dot{q}_2 \theta_\beta - \frac{\theta_Q}{V_2} + \Delta_{Q_2} \quad (9)$$

in which Q_{2M} can be thought as the control input.

Consider the following control law for Q_{2M}

$$Q_{2M} = (k_{p2} + k_{p2s}) \frac{V_2}{\theta_{\beta min}} e_{p2} + \frac{A_2}{V_2} \frac{\partial x_L}{\partial q_2} \dot{q}_2 - \frac{\hat{\theta}_Q}{\hat{\theta}_\beta} \quad (10)$$

where $\left(\frac{A_2}{V_2} \frac{\partial x_L}{\partial q_2} \dot{q}_2 - \frac{\hat{\theta}_Q}{\hat{\theta}_\beta} \right)$ represents the model

compensation term which will be denoted as Q_{2Ma} for short, $k_{p2} > 0$, and $k_{p2s} \geq 0$ is a nonlinear feedback gain chosen large enough to satisfy the following robust performance condition:

$$(i) \quad e_{p2} \left(-k_{p2s} \frac{\theta_\beta}{\theta_{\beta min}} e_{p2} + \phi_{p2}^T \tilde{\theta}_{p2} - \Delta_{Q_2} \right) \leq \varepsilon_p \quad (11)$$

$$(ii) \quad k_{p2s} \geq 0$$

where $\phi_{p2} = \left[\frac{A_2}{V_2} \frac{\partial x_L}{\partial q_2} \dot{q}_2 - \frac{Q_{2Ma}}{V_2}, -\frac{1}{V_2} \right]^T$. The parameter

adaptation law has the form of (7) with a positive definite diagonal adaptation rate matrix Γ_p and an adaptation function defined as:

$$\tau_p = \phi_{p2} \cdot e_{p2} \quad (12)$$

With the adaptive robust control law (10), it is shown in [22] that the following theoretical results hold:

A. In general, the offside pressure regulation is stable with a prescribed transient performance and

steady-state accuracy quantified by:

$$e_{p_2}^2(t) \leq e_{p_2}^2(0) \cdot \exp(-2k_{p_2}t) + \frac{\varepsilon_p}{k_{p_2}} [1 - \exp(-2k_{p_2}t)] \quad (13)$$

B. If after a finite time t_0 , $\Delta_{Q_2} = 0$, i.e., the model uncertainties are due to parametric uncertainties only, in addition to the result in A, asymptotic pressure tracking ($e_{p_2} \rightarrow 0$ as $t \rightarrow \infty$) is obtained for any positive gain k_{p_2} and ε_p .

3.3 Working-side Motion Controller Design

The boom motion dynamics and the cylinder pressure dynamics are described by (2) and (3). Define a set of parameters as $\theta = [\theta_1, \theta_2, \dots, \theta_6]^T$, $\theta_1 = 1/(1 + \ell_e^2 m_L / J_C)$, $\theta_2 = D_f / (J_C + m_L \ell_e^2)$, $\theta_3 = T_n / (J_C + m_L \ell_e^2)$, $\theta_4 = \beta_e$, $\theta_5 = \beta_e \tilde{Q}_{1n}$, and $\theta_6 = \beta_e \tilde{Q}_{2n}$, in which T_n , \tilde{Q}_{1n} , and \tilde{Q}_{2n} represent the nominal values of T , \tilde{Q}_1 , and \tilde{Q}_2 respectively. The system dynamic equations can thus be linearly parametrized as:

$$\begin{aligned} \ddot{q}_2 &= \frac{\theta_1}{J_C} \left[\frac{\partial x_L}{\partial q_2} (P_1 A_1 - P_2 A_2) - G_C \right] + \frac{\theta_1}{\ell_e^2} g \ell_g \\ &\quad - \ddot{q}_2 \theta_2 + \theta_3 - \frac{1}{\ell_e^2} g \ell_g + \Delta \\ \dot{P}_1 &= -\frac{A_1}{V_1} \frac{\partial x_L}{\partial q_2} \dot{q}_2 \theta_4 + \frac{\theta_4}{V_1} Q_{1M} + \frac{\theta_5}{V_1} + \Delta_{Q_1} \\ \dot{P}_2 &= \frac{A_2}{V_2} \frac{\partial x_L}{\partial q_2} \dot{q}_2 \theta_4 - \frac{\theta_4}{V_2} Q_{2M} - \frac{\theta_6}{V_2} + \Delta_{Q_2} \end{aligned} \quad (14)$$

where $\Delta = -(T_n - T) / (J_C + m_L \ell_e^2)$, $\Delta_{Q_1} = \beta_e (\tilde{Q}_{1n} - \tilde{Q}_1) / V_1$, and $\Delta_{Q_2} = \beta_e (\tilde{Q}_{2n} - \tilde{Q}_2) / V_2$. To illustrate the proposed adaptive robust motion controller design, this section presents a design procedure for those working modes during which the head end chamber is the working side, i.e., P_1 is the critical pressure to be precisely controlled for motion tracking. The motion controller design when P_2 is the working side chamber pressure follows the same procedure and is omitted.

Step 1

Define a switching-function-like quantity as

$$z_2 = \dot{z}_1 + k_1 z_1 = \dot{q}_2 - \dot{q}_{2r}, \quad \dot{q}_{2r} \triangleq \dot{q}_{2d} - k_1 z_1 \quad (15)$$

where $z_1 = q_2 - q_d(t)$ is the output tracking error with $q_d(t)$ being the reference trajectory. Differentiate (15) while noting (14):

$$\begin{aligned} \dot{z}_2 &= \theta_1 \left[\frac{1}{J_C} \left(\frac{\partial x_L}{\partial q_2} P_L - G_C \right) + \frac{1}{\ell_e^2} g \ell_g \right] - \frac{1}{\ell_e^2} g \ell_g \\ &\quad - \ddot{q}_{2r} - \theta_2 \dot{q}_2 + \theta_3 + \Delta \end{aligned} \quad (16)$$

If we treat P_L as the control input to (16), we can synthesize a virtual control law P_{Ld} such that z_2 goes to zero or as small as possible. Since (16) has both parametric uncertainties θ_1 through θ_3 and uncertain nonlinearity Δ , the ARC approach [19] can be used to deal with these model uncertainties effectively. The resulting control function P_{Ld} consists of two parts given by [22]:

$$\begin{aligned} P_{Ld}(q_2, \dot{q}_2, \hat{\theta}_1, \hat{\theta}_2, t) &= P_{Lda} + P_{Lds} \\ P_{Lda} &= \frac{\partial q_2}{\partial x_L} \left[G_C + \frac{J_C}{\hat{\theta}_1} \left(-\frac{\hat{\theta}_1}{\ell_e^2} g \ell_g + \hat{\theta}_2 \dot{q}_2 - \theta_3 + \frac{1}{\ell_e^2} g \ell_g + \ddot{q}_{2r} \right) \right] \\ P_{Lds} &= P_{Lds1} + P_{Lds2}, \quad P_{Lds1} = -\frac{J_C}{\theta_{1min}} \frac{\partial q_2}{\partial x_L} k_2 z_2 \end{aligned} \quad (17)$$

in which P_{Lda} functions as an adaptive model compensation, P_{Lds1} is a stabilizing control law with $k_2 > 0$, and P_{Lds2} is a feedback control law chosen to satisfy the following robust performance conditions [19]:

$$\begin{aligned} (i) \quad z_2 \left(\frac{1}{J_C} \theta_1 \frac{\partial x_L}{\partial q_2} P_{Lds2} - \tilde{\theta}^T \phi_2 + \Delta \right) &\leq \varepsilon_2 \\ (ii) \quad z_2 \frac{\partial x_L}{\partial q_2} P_{Lds2} &\leq 0 \end{aligned} \quad (18)$$

where ε_2 is a design parameter. If P_L were the actual control input, the adaptation function would be:

$$\begin{aligned} \tau_2 &= \phi_2 z_2 \\ \phi_2 &\triangleq \left[\frac{1}{J_C} \left(\frac{\partial x_L}{\partial q_2} P_{Lda} - G_C \right) + \frac{1}{\ell_e^2} g \ell_g, -\dot{q}_2, 1, 0, 0, 0 \right]^T \end{aligned} \quad (19)$$

Step 2

Denote $z_3 = P_L - P_{Ld}$ as the error between the actual load force and its desired value in (17). The goal of this step is to synthesize a virtual control flow so that z_3 converges to zero with a guaranteed transient performance and steady-state accuracy. From (14),

$$\begin{aligned} \dot{z}_3 &= \dot{P}_L - \dot{P}_{Ld} = -\left(\frac{A_1^2}{V_1} + \frac{A_2^2}{V_2} \right) \frac{\partial x_L}{\partial q_2} \dot{q}_2 \theta_4 + \frac{A_2}{V_2} \theta_4 Q_{2M} + \frac{A_1}{V_1} \theta_5 \\ &\quad + \frac{A_2}{V_2} \theta_6 - \dot{P}_{Ldc} + \frac{A_1}{V_1} \theta_4 Q_{1M} + A_1 \Delta_{Q_1} - A_2 \Delta_{Q_2} - \dot{P}_{Ldu} \end{aligned} \quad (20)$$

where:

$$\begin{aligned} \dot{P}_{Ldc} &= \frac{\partial P_{Ld}}{\partial q_2} \dot{q}_2 + \frac{\partial P_{Ld}}{\partial \dot{q}_2} \ddot{q}_2 + \frac{\partial P_{Ld}}{\partial t} \\ \dot{P}_{Ldu} &= \frac{\partial P_{Ld}}{\partial q_2} \left[-\frac{\tilde{\theta}_1}{J_C} \left(\frac{\partial x_L}{\partial q_2} P_L - G_C \right) - \frac{\tilde{\theta}_1}{\ell_e^2} g \ell_g(q_2) \right] \\ &\quad + \tilde{\theta}_2 \dot{q}_2 - \tilde{\theta}_3 + \Delta + \frac{\partial P_{Ld}}{\partial \hat{\theta}} \dot{\hat{\theta}} \end{aligned} \quad (21)$$

in which \hat{q}_2 represent the calculable part of \ddot{q}_2 given by:

$$\hat{q}_2 = \frac{\hat{\theta}_1}{J_C} \left(\frac{\partial x_L}{\partial q_2} P_L - G_C \right) + \frac{\hat{\theta}_1}{\ell_e^2} g \ell_g - \hat{\theta}_2 \dot{q}_2 + \hat{\theta}_3 - \frac{1}{\ell_e^2} g \ell_g \quad (22)$$

In (21), \dot{P}_{Ldc} is calculable and can be used in the construction of control functions, but \dot{P}_{Ldu} cannot due to various uncertainties. Therefore, \dot{P}_{Ldu} has to be dealt with via certain robust feedback in this step. In viewing (20), Q_{1M} can be thought as the control input for (20) and step 2 is to synthesize a control function Q_{1Md} for Q_{1M} such that P_L tracks the desired control function P_{Ld} synthesized in Step 1 with a guaranteed transient performance. Similar to (17), the control function Q_{1Md} consists of two parts given by:

$$\begin{aligned} Q_{1Md} &= Q_{1Mda} + Q_{1Mds} \\ Q_{1Mda} &= \frac{V_1}{A_1 \hat{\theta}_4} \left[-\frac{\hat{\theta}_1}{J_C} \frac{\partial x_L}{\partial q_2} z_2 + \hat{\theta}_4 \left(\left(\frac{A_1^2}{V_1} + \frac{A_2^2}{V_2} \right) \frac{\partial x_L}{\partial q_2} \dot{q}_2 \right. \right. \\ &\quad \left. \left. - \frac{A_2}{V_2} Q_{2M} \right) - \hat{\theta}_5 \frac{A_1}{V_1} - \hat{\theta}_6 \frac{A_2}{V_2} + \dot{P}_{Ldc} \right] \\ Q_{1Mds} &= Q_{1Mds1} + Q_{1Mds2}, \quad Q_{1Mds1} = -\frac{V_1}{A_1 \theta_{Amin}} k_3 z_3 \end{aligned} \quad (23)$$

where $k_3 > 0$. Similar to (18), Q_{1Mds2} is a robust control function chosen to satisfy the following robust performance conditions [22]:

$$\begin{aligned} (i) \quad & z_3 (\theta_4 Q_{1Mds2} - \tilde{\theta}^T \phi_3 - \frac{\partial P_{Ld}}{\partial \dot{q}_2} \Delta + A_1 \Delta_{Q_1} - A_1 \Delta_{Q_2}) \leq \varepsilon_3 \quad (24) \\ (ii) \quad & z_3 Q_{1Mds2} \leq 0 \end{aligned}$$

where ε_3 is a positive design parameter. The adaptation function would be

$$\tau = \tau_2 + \phi_3 z_3 \quad (25)$$

where ϕ_3 is defined as:

$$\phi_3 \triangleq \begin{bmatrix} \frac{1}{J_C} \frac{\partial x_L}{\partial q_2} z_2 - \frac{\partial P_{Ld}}{\partial \dot{q}_2} \left[\frac{1}{J_C} \left(\frac{\partial x_L}{\partial q_2} P_L - G_C \right) + \frac{1}{\ell_e^2} g \ell_g \right] \\ \frac{\partial P_{Ld}}{\partial \dot{q}_2} \dot{q}_2 \\ - \frac{\partial P_{Ld}}{\partial \dot{q}_2} \\ - \left(\frac{A_1^2}{V_1} + \frac{A_2^2}{V_2} \right) \frac{\partial x_L}{\partial q_2} \dot{q}_2 + \frac{A_2}{V_2} Q_{2M} + \frac{A_2}{V_2} Q_{1Ma} \\ \frac{A_1}{V_1} \\ \frac{A_2}{V_2} \end{bmatrix} \quad (26)$$

With the adaptive robust control law (23) and the projection type adaptation law (7) with adaptation function (25) for θ , the following results hold [22]:

A. In general, the overall closed loop system is stable with a prescribed transient performance and final tracking accuracy quantified by:

$$V_3(t) \leq V_3(0) \cdot \exp(-2\lambda t) + \frac{\varepsilon}{2\lambda} [1 - \exp(-2\lambda t)] \quad (27)$$

where $V_3(t) = \frac{1}{2} \sum_{i=2}^3 k_i z_i^2$, $\lambda = \min\{k_2, k_3\}$, $\varepsilon = \varepsilon_2 + \varepsilon_3$

B. If after a finite time t_0 , $\Delta = 0$ and $\Delta_{Q_i} = 0, i=1,2$, in addition to the results in A, asymptotic motion tracking ($z_i \rightarrow 0$ as $t \rightarrow \infty$) is obtained for any positive gain $k_i, k=1,2,3$ and $\varepsilon_i, i=2,3$.

4 Comparative Experiments

Experiments have been done to test the proposed two-level control system. The programmable valves were used to control the boom motion of the electro-hydraulic arm to track a desired motion trajectory for up and down motions shown in Fig. 10. The programmable valves were compared in terms of motion tracking performance as well as energy usage with a critically centred servo valve and a close-centred PDC valve with the direct deadband inverse compensation using the same baseline ARC motion controller [20].

The tracking performances of the three systems were plotted in Fig. 11 and quantified in Table 3 using the following three indexes: (1) $\|e\|_1$ defined as $\int_0^{20} |e(t)| dt$; (2) $\|e\|_2$ defined as $\int_0^{20} e^2(t) dt$; and (3) $\|e\|_\infty$ defined as $\max|e(t)|$.

Table 3: Comparison of Tracking Errors

| Value | $\ e\ _1$ | $\ e\ _2$ | $\ e\ _\infty$ |
|--------------|-----------|-----------|----------------|
| PDC | 0.0030 | 0.0046 | 0.0146 |
| Servo | 0.0014 | 0.0018 | 0.0051 |
| Programmable | 0.0007 | 0.0010 | 0.0036 |

As seen from these results, all three systems exhibit good tracking performance as their maximum tracking errors are all less than 0.015 rad. As expected, the servo valve has a smaller tracking error when compared to the PDC valve; the PDC valve has significantly larger transient errors at the beginning and the end of each travel when the deadband effects are most severe. The proposed

programmable valves do not have this deadband issue and in fact achieve an even better tracking performance when compared to the very expensive servo valve; such a performance gain may come from the fact that the cartridge valves have really fast response due to the smaller inertia of the poppet.

A comparison of cylinder working pressures of each system is shown in Fig. 12. The cylinder pressures in the system controlled by the programmable valves are much lower than the pressures in the other two systems, with one chamber pressure always close to the tank pressure, a preset pressure of 200KPa to compensate for the line loss and to prevent cavitations. This is due to the result of the decoupled control of cylinder pressures which are made possible by the proposed programmable valves.

The power usages of the three systems are shown in Fig.13. The experiment setup used a pump with a constant supplied pressure of 6900KPa (1000PSI). As seen, during the upward motion periods (roughly, 1 through 3.5 seconds and 11 through 13.5 seconds in the figures), the three systems use almost the same amount of energy as pump flow is needed to lift the payload. However, during the downward motion periods (roughly, 6 through 8.5 seconds and 16 through 18.5 seconds in the figures), the programmable valves controlled system did not use any pump energy at all due to the use of regeneration flow for precise cylinder motion controls, while the other two systems still need pump flows for a controlled downward motion. It is worth noting that the proposed programmable valves not only enable the use of regeneration flow to reduce energy consumption but also the precise control of regeneration flow for a well controlled motion – the resulting motion tracking error shown in Fig. 11 is even better than that is achieved by a servo valve. Such a use of regeneration flow is much different from existing energy saving systems [1,7] where the regeneration flows are not precisely controlled and only coarse motions such as the free falls can be performed. In addition, the programmable valves controlled system uses about 2/3 of energy consumed by the other systems; the total pump energy used by three systems for this specific task were 32.4KJ and 32.7KJ for PDC and servo systems, respectively, and only 21.3KJ for the programmable valves system.

In mobile hydraulic industry, instead of a constant supplied pressure pump, a load sensing pump (i.e., the pump supplied pressure is varied according to the required cylinder chamber pressures) is normally used for further energy saving [1]. When a load sensing pump is available, much more energy saving can be obtained with the proposed programmable valves due to the significantly reduced cylinder working pressures shown in Fig.12. Unfortunately, our experimental setup does not have a load sensing pump and it is impossible to experimentally test the three valves with a load sensing pump. Instead, a virtual comparison is done to mimic a load sensing pump by adding 500KPa to the cylinder working pressure connected to the pump as the pump supplied pressure. With this assumption, the comparative results for pump power usage of three systems are shown in Fig.14, in which the programmable valve controlled system uses about only 1/3 of the energy consumed by the other two systems.

5 Conclusions

The paper revisits recent research on the precision and energy saving control of electro-hydraulic systems from an integrated mechatronic design perspective. It is shown that through a seamless integration of the new physical capabilities gained by novel hardware redesign (e.g., the proposed programmable valves) and the advanced adaptive robust controls, traditionally conflicting requirements of lower cost, higher performance, and less energy consumptions could be simultaneously achieved. Such an integrated mechatronic design philosophy has also been successfully tested through comparative experiments.

Acknowledgement

The work is supported in part by the US National Science Foundation (Grant No. CMS-0600516) and in part by the National Natural Science Foundation of China (NSFC) under the Joint Research Fund for Overseas Chinese Young Scholars (Grant No.50528505).

References

- [1] J.A. Aardema and D.W. Koehler, System and method for controlling an independent metering valve, **United States Patent**, 5,947,140, 1999.
- [2] A. Alleyne and J. K. Hedrick, Nonlinear adaptive control of active suspension, **IEEE Trans. on Control Systems Technology**, vol.3, no. 1, 94–101, 1995.
- [3] R. Book and C.E. Goering, Programmable electrohydraulic valve, **SAE Transactions**, vol.108, no. 2, 346–352, 1999.
- [4] Fanping Bu and Bin Yao, Adaptive robust precision motion control of single-rod hydraulic actuators with time-varying unknown inertia: A case study, **Proc. of ASME International Mechanical Engineering Congress and Exposition**, vol. FPST-6, pp. 131–138, Nashville, TN, 1999
- [5] Fanping Bu and Bin Yao, Nonlinear adaptive robust control of hydraulic actuators regulated by proportional directional control valves with deadband and nonlinear flow gain coefficients, **Proc. of American Control Conference**, pp. 4129–4133, Chicago, IL, 2000.
- [6] Joel D. Fortgang, Lynne E. George, and Wayne J. Book, Practical implementation of a dead zone inverse on a hydraulic wrist, **Proc. of ASME International Mechanical Engineering Congress and Exposition**, IMECE 2002-39351, New Orleans, LA, 2002,
- [7] K.D. Garnjost, Energy-conserving regenerative-flow valves for hydraulic servomotors, **United States Patent**, 4,840,111, 1989.
- [8] A. Jansson and J.-O. Palmberg, Separate control of meter-in and meter-out orifices in mobile hydraulic systems, **SAE Transactions 99 (1990)**, no. 2, 337–383.
- [9] K.D. Kramer and E.H. Fletcher, Electrohydraulic valve system, **United States Patent**, Re. 33,846, 1990.
- [10] Song Liu and Bin Yao, Energy-saving control of single-rod hydraulic cylinders with programmable valves and improved working mode selection, **SAE Transactions - Journal of Commercial Vehicle**, SAE 2002-01-1343, pp.51–61, 2002.
- [11] Song Liu and Bin Yao, Automated modelling of cartridge valve flow mapping, **IEEE/ASME Transactions on Mechatronics**, vol. 11, no. 4, pp. 381–388, 2006. Winner of the Best Student Paper Award in **IEEE/ASME International conference on Advanced Intelligent Mechatronics (AIM) (Monterey, CA)**, pp. 789-794, 2005.
- [12] Song Liu and Bin Yao, Characterization and attenuation of sandwiched deadband problem using describing function analysis and its application to electro-hydraulic systems controlled by closed-center valves, **Proc. of the ASME International Mechanical Engineers Congress and Exposition (IMECE)**, IMECE2004-60946, 2004. The revised version is in press for *the ASME J. of Dynamic Systems and Control*, 2009.
- [13] Herbert E. Merritt, Hydraulic control systems, **John Wiley & Sons**, 1967.
- [14] Gang Tao and Petar V. Kokotovic, Adaptive control of systems with actuator and sensor nonlinearities, **John Wiley & Sons, Inc**, 1996.
- [15] A. Taware and G. Tao, Control of Sandwich Nonlinear Systems. Berlin: Springer-Verlag, 2003.
- [16] Thomas J. Ulery, Proportional cartridge valves - economical alternative to large valves, **Agricultural Engineering 71 (1990)**, no. 4, 11.
- [17] J. Watton, Fluid power systems, **Prentice Hall**, 1989.
- [18] Li Xu and Bin Yao, Adaptive robust precision motion control of linear motors with negligible electrical dynamics: Theory and experiments, **Proc. of American Control Conference**, pp. 2583–2587, Chicago, IL, 2000, The revised full version appeared in the **IEEE/ASME Trans. on Mechatronics**, vol.6, no.4, pp.444-452, 2001.
- [19] Bin Yao, High performance adaptive robust control of nonlinear systems: a general framework and new schemes, **Proc. of IEEE Conference on Decision and Control**, pp. 2489–2494, 1997.
- [20] Bin Yao, Fanping Bu, John T. Reedy, and George T.C. Chiu, Adaptive robust control of single-rod hydraulic actuators: Theory and experiments, **IEEE/ASME Trans. on Mechatronics**, vol.5, no. 1, 79–91, 2000.
- [21] Bin Yao and C. Deboer, Energy-saving adaptive robust motion control of single-rod hydraulic cylinders with programmable valves, **Proc. of**

American Control Conference, pp. 4819–4824, 2002.

- [22] S. Liu and B. Yao, Coordinate control of energy saving programmable valves,” **IEEE Transactions on Control System Technology**, vol. 16, no. 1, pp. 34–45, 2008.

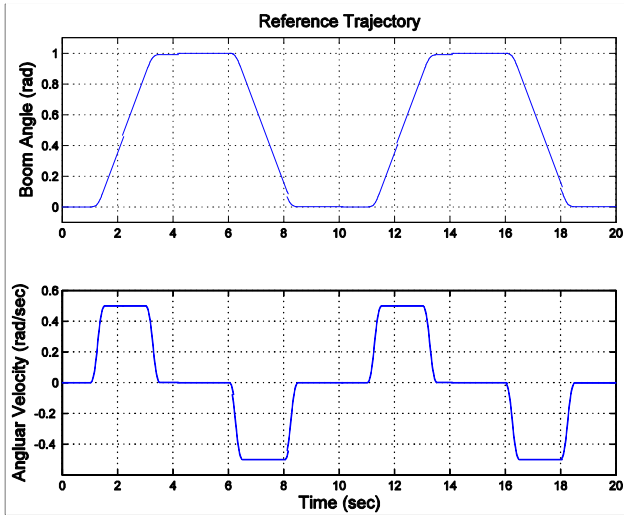


Fig. 10: Desired trajectory for up and down motions

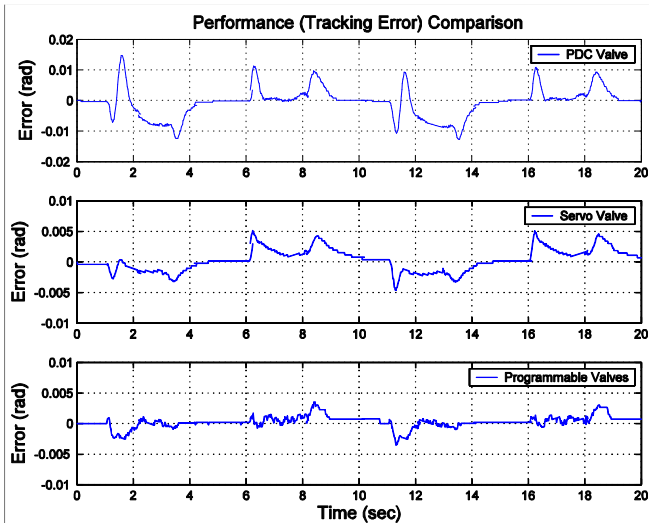


Fig.11: Tracking performance comparison

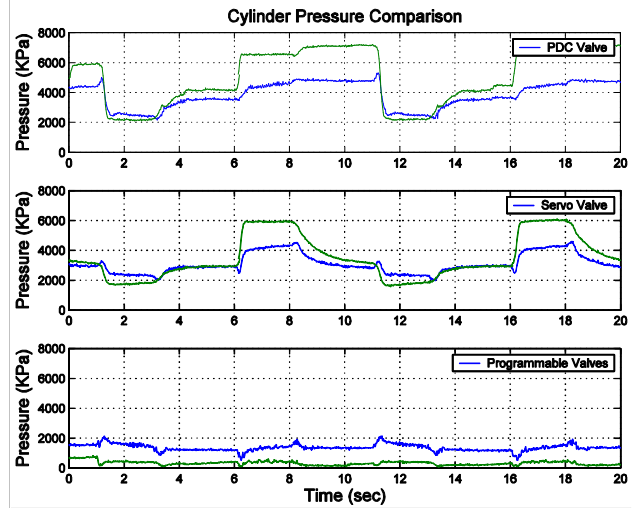


Fig. 12: Cylinder working pressures comparison

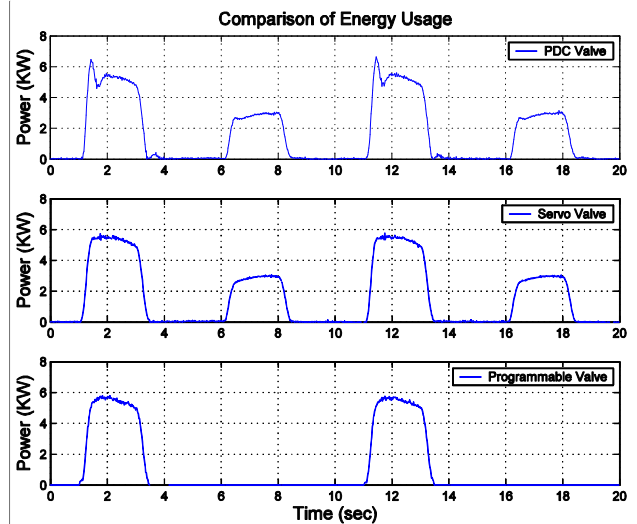


Fig. 13: Energy usages (fixed supplied pressure pump)

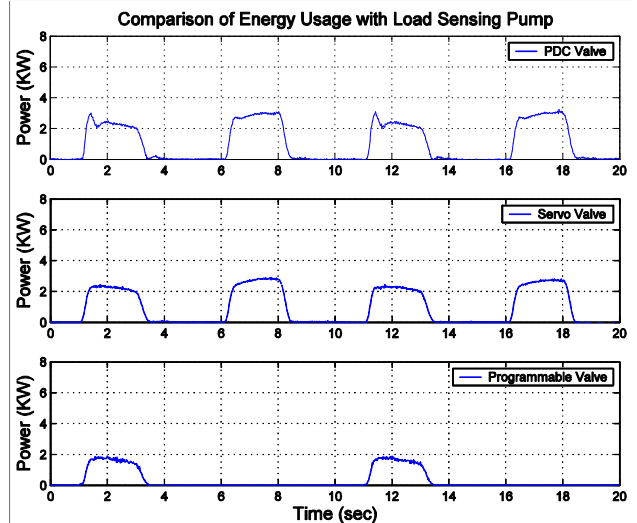


Fig. 14: Energy usages (load sensing pump)